ISSN 1024-588X. Вісник Львівського університету. Серія фізична. 2020. Випуск 57. С. 101-113
Visnyk of the Lviv University. Series Physics. 2020. Issue 57. P. 101-113

УДК 538.915; 621.315.592 https://doi.org/10.30970/ph.57.2020.101
PACS 71.20.Nr, 71.15.Ap, 42.70.Nq

Electronic band structures of $Si_{1-x}Ge_x$, $Si_{1-x}Sn_x$ and $Ge_{1-x}Sn_x$ semiconductor alloys

P.M. Yakibchuk, O.V. Bovgyra, M.V. Kovalenko, I.V. Kutsa

Ivan Franko National University of Lviv
Kyrylo and Mefodiy St, 8, 79005 Lviv, Ukraine
e-mail: oleh.bovhyra@lnu.edu.ua

We used the model pseudopotential calculations to investigate the band structures of group-IV semiconductor alloys, including $Si_{1-x}Ge_x$, $Si_{1-x}Sn_x$ and $Ge_{1-x}Sn_x$. The calculations of electronic properties for $Si_{1-x}Ge_x$ alloys demonstrate the reliability of the method we used. For $Ge_{1-x}Sn_x$, the direct band gap optical bowing parameter we obtained is 2.74 eV and the indirect–direct band gap crossover is at $x = 0.068$, both consistent with the existing experimental data. The calculated indirect-direct band gap change point in $Si_{1-x}Sn_x$ alloys is found close to approximately tin content $x = 0.6$. The corresponding energy gap is 0.75 eV, which is suitable for the on-chip optoelectronical devices.

Key words: model pseudopotential, band structure, semiconductors

1. Introduction

Elemental semiconductors silicon and germanium form a wide series of alloys containing Sn with interesting applications in various optoelectronic devices [1]. In semiconductor alloys, the band gap value and the lattice parameter are among the most important physical parameters, since these parameters control the band off-set and the mismatching in the different devices. A full range of technological advances are expected if it becomes possible to achieve semiconductors with any desired bandgap that can be adapted to specific applications. The bandgaps range that can be achieved in bulk crystalline alloys is practically limited by the strict requirement of the lattice matching in planar epitaxial growth. The larger tolerance to lattice mismatch at the nanoscale allows semiconductor alloy nanomaterials provide new opportunities for bandgap engineering.

The progress in epitaxial growth of GeSn and SiGeSn alloys paved the way toward direct bandgap optoelectronic devices as well as GeSn-based nanoelectronics with an enormous potential speciffically regarding monolithic integration. Alloys and ordered compounds of Si-Ge-Sn group have particularly unique optoelectronic properties for applications in quantum-well intersubband technology, MOSFET and n-FET devices

[2–4]. The demonstration of lasing in Si-Ge-Sn alloys can be seen as a breakthrough in group IV photonics [5].

Direct and indirect energy gaps, electron and hole effective masses as well as their composition dependences are the most critical parameters for band-structure calculations of tin based group IV semiconductor alloys. Therefore, an accurate knowledge of these parameters for binary $Si_{1-x}Sn_x$ and $Ge_{1-x}Sn_x$, ternary $Ge_{1-x-y}Si_xSn_y$ is very important. Moreover, calculation of band offsets for $Ge_{1-x-y}Si_xSn_y$ is useful for calculating the energy bands in quantum heterostructures. The bandgaps range that can be achieved in bulk crystalline alloys is practically limited by the strict requirement of the lattice matching in planar epitaxial growth. Also the larger tolerance to lattice mismatch at the nanoscale allows semiconductor alloy nanomaterials provide new opportunities for bandgap engineering.

2. Calculation method

There are many theoretical studies devoted to simulation of the band structures of binary $Ge_{1-x}Sn_x$ [6–14], $Si_{1-x}Sn_x$ [15–17] and ternary $Ge_{1-x-y}Si_xSn_y$ [18–23] compounds using various approaches like the empirical pseudopotential method, tight binding, the **kp** method and density functional theory (DFT) based methods.

Most of the reports cover only a limited composition range and the full range composition dependence of the band structure and band offsets is absent. The significant inconsistency in the reports data is observed for some properties, like the composition dependences of the band gaps, the threshold of Sn content causing indirect – direct crossover, the dependence of the energy gaps on the atomic distribution and the band offsets in the alloys.

For example, in case of $Si_{1-x}Sn_x$ alloys several theoretical reports have predicted that the indirect – direct crossover in will occur at values from x = 0.25 to 0.67, depending on the calculation method [15–17, 19]. This dissimilarity in the results is mainly due to the difficulty of handling the randomness in alloy systems.

For $Ge_{1-x}Sn_x$ alloy it has been clearly demonstrated that the electronic band structure can be tuned from indirect to direct band gap as well as an inverted band gap structure [12].

To help understand behaviour of bowing and related properties of the materials, we performed a calculation of the electronic band parameters for series $Si_{1-x}Sn_x$ semiconductor alloys. For this purpose, we have used model and ab initio pseudopotential plane wave methods within the mixed-atom supercell model of alloys. First principles calculations generally underestimate the band gap energies and require substantial computational time. The issue of band gap underestimation also becomes worse for narrow band gap materials, such as $Si_{1-x}Sn_x$ alloy.

In this study, for band structure calculation of semiconductor alloys in Si-Ge-Sn system, we used the model pseudopotential (MP) plane wave method, which can predict the band structure of semiconductors with good accuracy [24–26].

Also, for geometry optimization the ab initio DFT calculations were performed using the sX-LDA formalism in conjunction with a 5x5x5 Monkhorst-Pack grid in the first Brillouin zone and a 500 eV energy cutoff. The cell dimensions and atomic positions were

optimized to yield the ground state crystalline structures.

The cell dimensions and atomic positions were optimized to yield the ground state crystalline structures. Our calculated equilibrium lattice constants are 5.461 Åfor Si and 6.657 Åfor α-Sn, which are consistent with previously reported experimental data and theoretical results. For the $Si_{1-x}Ge_x$, $Si_{1-x}Sn_x$ and $Ge_{1-x}Sn_x$ alloys the lattice constants vary with concentration parameter x. The lattice constants of considered alloys were determined using the Vegard expression,

$$a_{AB} = a_A x + a_B(1-x) + bx(1-x). \tag{1}$$

The electronic band structures were determined by the relative positions of the minimum conduction band at the Γ-, X-, and L-points in the first Brillouin zone. In this study, we model a series of 8-atom unit cells of the $Si_{1-x}Ge_x$ and $Si_{1-x}Sn_x$ alloys (where discrete Ge(Sn) compositions of 12.5%, 25%, 37.5%, 50%, 62.5%, 75%, and 87.5% or x = 0.125, 0.25, 0.375, 0.5, 0.625, 0.75, and 0.875), in which Si, Ge and Sn are distributed on the various substitutional sites to form alloy structures as homogeneous alloys.

3. Results and discussion

3.1 $Si_{1-x}Ge_x$ alloys

To show that the method we used is reliable we start our studies from the $Si_{1-x}Ge_x$ alloy, which has been investigated intensively. The lattice constant bowing obtained for unstrained $Si_{1-x}Ge_x$ is b = 0.026 Å.

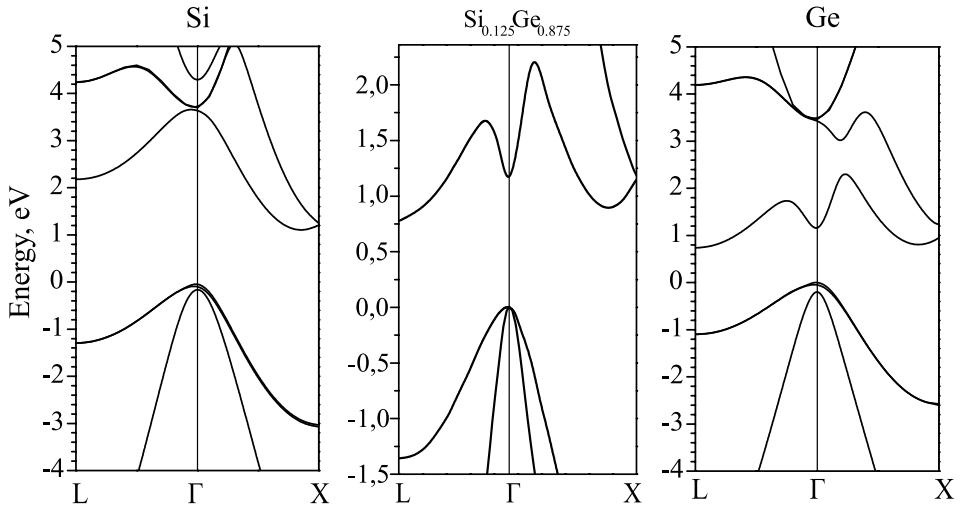

Fig. 1: Electronic band structures of $Si_{1-x}Ge_x$ along L-Γ-X path for (a) x = 0, (b) x = 0.875, and (c) x = 1.0, showing the band gap crossover.

Germanium is fundamentally an indirect band gap semiconductor. The indirect energy gap, $E_g(L)$ = 0.664 eV at 300 K, is between the highest valence band state

at Γ point and the lowest conduction band states at L high-symmetry piont, which lies 0.136 eV above the conduction band minimum. The bandstructure of bulk Ge is presented in Fig. 1 together with band structures of pure Si and $Si_{0.125}Ge_{0.875}$ alloy.

Supercell approaches used to calculate the electronic properties of considered alloys produce accurate, but folded, band structures. Using an optimized algorithm, we unfold the band structure to an approximate $E(k)$ relation associated with an effective Brillouin zone. We must indicate that the effect of the atom displacement in alloys on its electronic properties, to consider the structural relaxation is very important for the band calculation. The band diagrams of $A_{8-n}B_n$ structural models were calculated for all atomic configurations with the geometrical relaxation. Then, the calculated results for band gap values E_g were averaged by considering the formation probability of each point.

From Fig.1 it is realizable to see a band gap crossover in $Si_{1-x}Ge_x$ where the conduction band minimum moves from L to X(Δ) valley as the Si concentration increases. The corresponding band gaps values are plotted versus Ge concentration x in Fig. 2, and band gap crossover occur at value of $x = 0.86$.

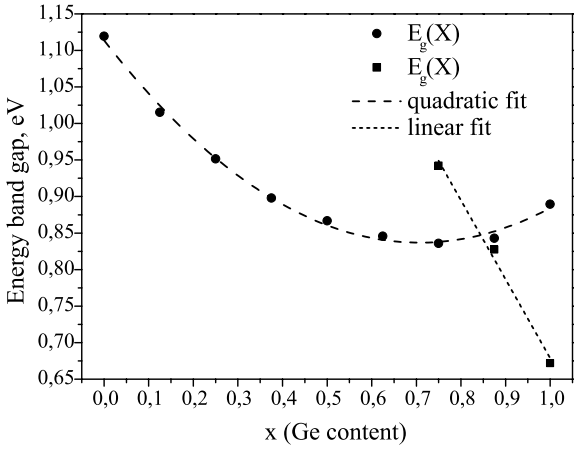

Fig. 2: Band gaps of the $Si_{1-x}Ge_x$ alloy as a function of Ge concentration.

Experimental results measured at low temperatures separated the band gap of $Si_{1-x}Ge_x$ into linear and quadratic ranges and obtained the crossover at $x = 0.85$ by the fitting process [27]. At this crossover point, the conduction band minima at L and X(Δ) valleys have the same energy, as shown in the band structure. The band gap bowing of the quadratic region is 0.235 eV, which excellently agrees with experiment values for the $Si_{1-x}Ge_x$ alloy. These results show that the method we used is reliable and correct.

3.2 $Si_{1-x}Sn_x$ alloys

Whereas crystalline Si and Ge are semiconductors with diamond cubic lattices and strong covalent bonds, Sn is an allotropic element that passes a phase transition from its semiconducting α-Sn phase with diamond cubic lattice structure to a metallic β-Sn phase with a body-centered tetragonal structure. Moreover, the crystalline bonds of the α-Sn phase are not strong covalent but rather at the boundary between covalent and metallic.

The analysis of α-Sn electronic properties are essential to predict the characteristics of its alloys with Si and Ge.

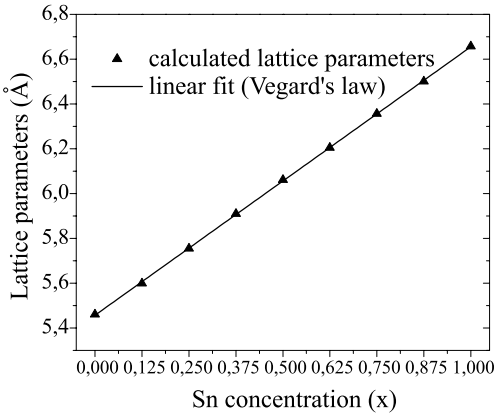

Fig. 3: Compositional dependence of lattice parameters in $Si_{1-x}Sn_x$ alloys.

Fig. 3 shows lattice parameters related to the pure silicium, isotropic $Si_{1-x}Sn_x$ arrangements of the intermediate compositions, and α-Sn. The strong linear relation between lattice parameters and composition of $Si_{1-x}Sn_x$ alloys exhibits Vegard behavior, yielding a bowing coefficient $b = 0.084$ Å. The Si and Sn atoms are displaced from the initial position in a diamond lattice structure by strain relaxation due to the difference in atomic radius between them.

Calculated band structures for $Si_{1-x}Sn_x$ alloys with Sn concentration as 37.5%, 50%, and 62.5% are shown in Figs. 4(a)–4(c), respectively. Fig. 4 shows the indirect to direct band gap transition for $Si_{1-x}Sn_x$. A closer inspection of changes in the band structure upon increased Sn incorporation reveals that as the direct band gap shrinks, the electron and hole valleys at Γ point become narrower. Thus, as Sn content in $Si_{1-x}Sn_x$ increases, effective masses at Γ point decreases for both electrons and holes.

The band gap energy of $Si_{1-x}Sn_x$ at X, L, and Γ points obtained from the band structures calculated by MP is plotted against Sn compositions in Fig. 5. On Fig. 5 we also plot experimental value of indirect gap around $x = 0.18$ [28]. We can see that the band gaps values at Γ and L points decrease with increasing Sn content. The dependence of the X-point band gap on Sn compositions exhibits a simplest linear function relation with a correlation coefficient of 0.79754. In contrast, the L-point band gaps are highly sensitive to Sn compositions.

The calculated indirect-direct band gap crossover in $Si_{1-x}Sn_x$ alloys is found close to approximately tin content $x = 0.6$, which is extracted from appropriate curve-fitting of Γ and L valley band gaps. The corresponding energy gap is $E_g = 0.75$ eV, which is suitable for the on-chip optoelectronical devices.

3.3 $Ge_{1-x}Sn_x$ alloys

The present discussion in the literature regarding the band gap evolution of GeSn alloys is based on the assumption that with increasing Sn composition there is a sharp

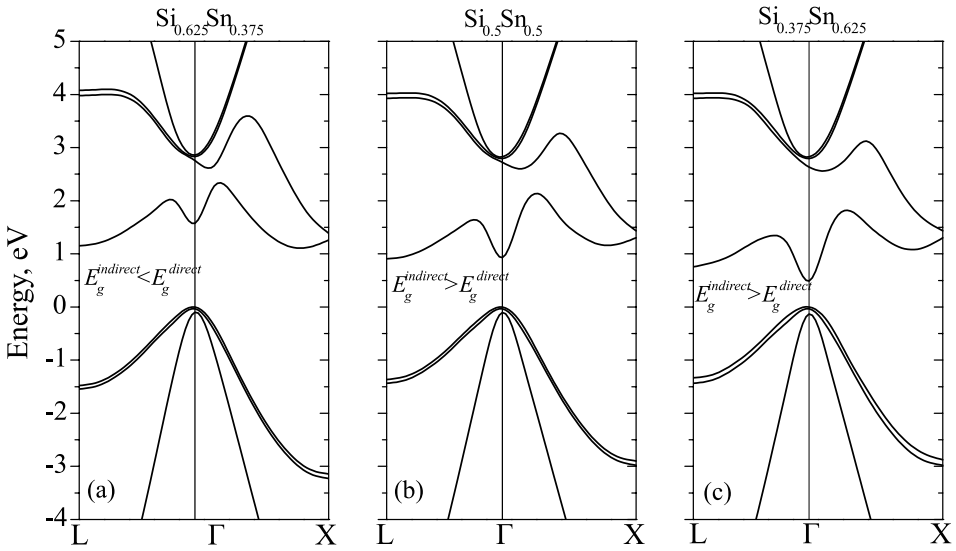

Fig. 4: Electronic band structures of $Si_{1-x}Sn_x$ along L-Γ-X path for (a) $x = 0.375$, (b) $x = 0.50$, and (c) $x = 0.625$, showing the transition from indirect to direct band gap.

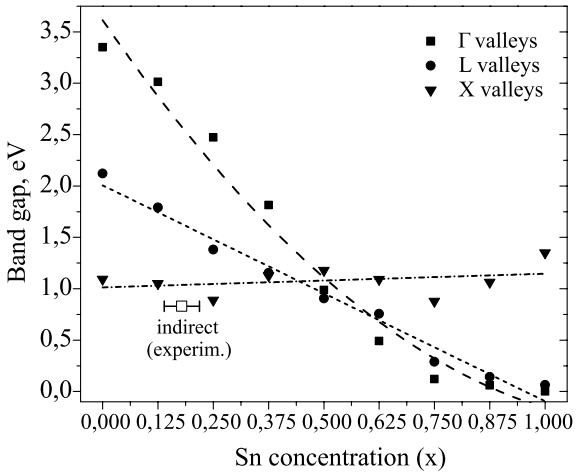

Fig. 5: The calculated band gap energies of L, Γ and X-point at various Sn compositions in $Si_{1-x}Sn_x$ alloy.

transition from GeSn being an indirect band gap material to a direct one. However, there is a large degree of uncertainty for the Sn concentration at which this transition occurs, with typical values ranging from 6–11% Sn.

To achieve a lower critical Sn concentration for the indirect–direct band gap transition, we study the band structure of non-strained $Ge_{1-x}Sn_x$ alloy with the supercells consisting of 32 atoms. The strong linear relation between lattice parameters and composition of

$Ge_{1-x}Sn_x$ alloys exhibits Vegard behavior, yielding a bowing coefficient $b = 0.109$ Å. The calculated bowing coefficient is consistent with the reported experimental observation ($b = 0.166$ Å).

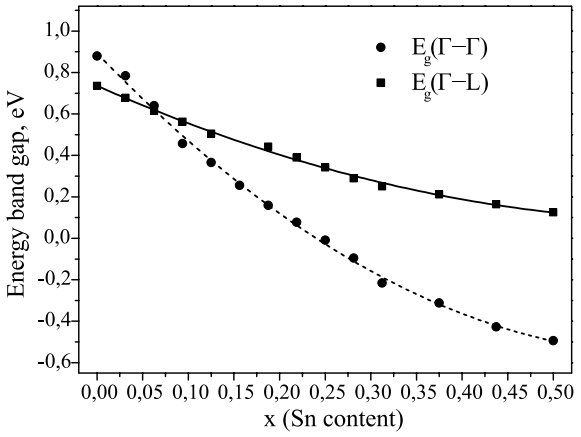

Fig. 6: Band gaps of the $Ge_{1-x}Sn_x$ alloy as a function of Sn concentration.

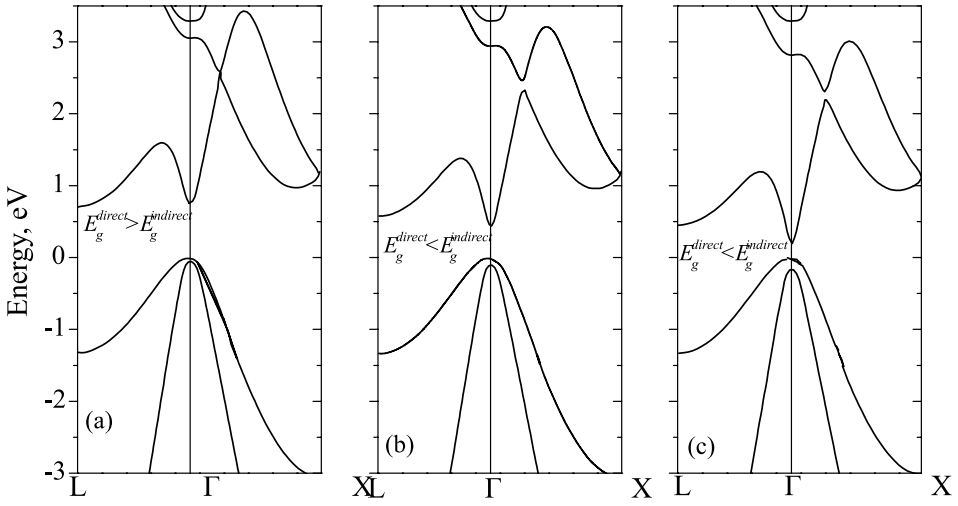

Fig. 7: Electronic band structures of $Ge_{1-x}Sn_x$ along L-Γ-X path for (a) $x = 0.03125$, (b) $x = 0.09375$, and (c) $x = 0.25$, showing the transition from indirect to direct band gap.

The most pronounced changes in the alloy electronic structure are occurring in the conduction band, especially around the Γ point. In Fig. 6, we present the indirect (Γ–L) and direct (Γ–Γ) band gaps of this system versus Sn concentration. The crossover of the indirect and direct band gaps of an unstrained system is located at $x = 0.068$, where the conduction band minimum moves from L to Γ valley as shown in Fig. 7, i.e., an indirect–direct band gap transition occurs. This result is in agreement with the recent

calculations using a supercell method and full-zone 30-band k·p model [29].

The four characteristic regions of the composition dependence can be distinguished: an in-direct band gap (0–6.8% Sn), a direct band gap (6.8–25% Sn) and an inverse band gap semiconductor (Sn $>$ 25%). The direct band gap behavior as a function of concentration view a slightly non-parabolic character. The obtained value of the bowing parameter is $b = 2.74$ eV.

The comparison of theoretical calculations performed in this work with the available experimental data show that energies of direct optical transition determined from reflectance measurements [30] agree very well with obtained direct band gap value in $Ge_{1-x}Sn_x$.

Conclusions

In summary, we present a model pseudopotential method to calculate the electronic band structure properties of SiGe, SiSn and GeSn alloys. The band gap transition point in $Si_{1-x}Ge_x$ (at 14% of Si content) from X to L type is correctly predicted.

Obtained results reveal that by increasing the Sn content, the $Si_{1-x}Sn_x$ alloys could become a direct band-gap material, which would be quite beneficial in the field of Si photonics. The calculated indirect-direct band gap crossover in $Si_{1-x}Sn_x$ alloys is found close to approximately tin content $x = 0.6$. The corresponding energy gap is 0.75 eV, which is suitable for the on-chip optoelectronic devices.

For $Ge_{1-x}Sn_x$, the direct band gap optical bowing parameter we obtained is 2.74 eV and the indirect–direct band gap transition point is at $x = 0.068$, both consistent with the existing experimental data.

The obtained results lay a foundation for further investigations on electronic structure, electrical and/or optical properties, quantum device simulations, and applications of SiGeSn semiconductor alloys.

1. Soref R.A. Silicon-based Group IV Heterostructures for Optoelectronic Applications / R.A. Soref // Journal of Vacuum Science & Technology A: Vacuum, Surfaces, and Films. – 1996. – Vol. 14. – P. 913–918. doi:10.1116/1.580414.
2. Kouvetakis J. Tin-based group IV semiconductors: New Platforms for Opto- and Microelectronics on Silicon / J. Kouvetakis, J. Menendez, A.V.G. Chizmeshya // Annu. Rev. Mater. Res. – 2006. – Vol. 36 (1). – P. 497–554. doi:10.1146/annurev.matsci.36.090804.095159.
3. Ionescu A. M. Tunnel Field-Effect Transistors as Energy-Efficient Electronic Switches / A.M. Ionescu, H. Riel // Nature. – 2011. – Vol. 479 (7373). – P. 329–337. doi:10.1038/nature10679.
4. Schulte-Braucks C. Process Modules for GeSn Nanoelectronics with High Sn-Contents / C. Schulte-Braucks, S. Glass, E. Hofmann et al. // Solid-State Electronics. – 2017. – Vol. 128. – P. 54–59. doi:10.1016/j.sse.2016.10.024.
5. Wirths S. Si–Ge–Sn Alloys: From Growth to Applications / S. Wirths, D. Buca, S. Mantl // Progress in Crystal Growth and Characterization of Materials. – 2016. – Vol. 62 (1). – P. 1–39. doi:10.1016/j.pcrysgrow.2015.11.001.

6. Shen J. Ab Initio Calculation of the Structure of the Random Alloys $Sn_{1-x}Ge_x$ / J. Shen, J. Zi, X. Xie, P. Jiang // Phys. Rev. B. – 1997. – Vol. 56 (19). – P. 12084–12087. doi:10.1103/PhysRevB.56.12084.
7. Alberi K. Band Anticrossing in Highly Mismatched $Sn_{1-x}Ge_x$ Semiconducting Alloys / K. Alberi, J. Blacksberg, L.D. Bell et al. // Phys. Rev. B. – 2008. – Vol. 77 (7). – P. 073202. doi:10.1103/PhysRevB.77.073202.
8. Pulikkotil J. J. Structure of $Sn_{1-x}Ge_x$ Random Alloys as Obtained from the Coherent Potential Approximation / J.J. Pulikkotil, A. Chroneos, U. Schwingenschlogl // Journal of Applied Physics. – 2011. – Vol. 110 (3). – P. 036105. doi:10.1063/1.3618671.
9. Lu Low K. Electronic Band Structure and Effective Mass Parameters of $Sn_{1-x}Ge_x$ Alloys / K. Lu Low, Y. Yang, G. Han, W. Fan, Y.-C. Yeo // Journal of Applied Physics. – 2012. Vol. 112 (10). – P. 103715. doi:10.1063/1.4767381.
10. Lee M.-H. Electronic Band Structures of $Ge_{1-x}Sn_x$ Semiconductors: A First-Principles Density Functional Theory Study / M.-H. Lee, P.-L. Liu, Y.-A. Hong et al. // Journal of Applied Physics. – 2013. – Vol. 113 (6). – P. 063517. doi:10.1063/1.4790362.
11. Wang X. A Hybrid Functional First-Principles Study on the Band Structure of Non-Strained $Ge_{1-x}Sn_x$ Alloys / X. Wang, C. Chen, S. Feng, X. Wei, Y. Li // Chinese Phys. B. – 2017. – Vol. 26 (12). – P. 127402. doi:10.1088/1674-1056/26/12/127402.
12. Polak M. P. The Electronic Band Structure of $Ge_{1-x}Sn_x$ in the Full Composition Range: Indirect, Direct, and Inverted Gaps Regimes, Band Offsets, and the Burstein–Moss / M.P. Polak, P. Scharoch, R. Kudrawiec // Effect. J. Phys. D: Appl. Phys. – 2017. – Vol. 50 (19). – P. 195103. doi:10.1088/1361-6463/aa67bf.
13. Cho Y. First-Principle Study for More Accurate Optical and Electrical Characterization of $Ge_{1-x}Sn_x$ Alloy for Si and Group-IV Device Applications / Y. Cho, S. Cho, B.-G. Park, J.S. Harris // JSTS. – 2017. – Vol. 17 (5). – P. 675–684. doi:10.5573/JSTS.2017.17.5.675.
14. Eales T. D. $Ge_{1-x}Sn_x$ Alloys: Consequences of Band Mixing Effects for the Evolution of the Band Gap ?-Character with Sn Concentration / T.D. Eales, I.P. Marko, S. Schulz et al. // Sci. Rep. – 2019. – Vol. 9 (1). – P. 14077. doi:10.1038/s41598-019-50349-z.
15. Tolle J. Temperature Chemical Vapor Deposition of Si-Based Compounds via SiH3SiH2SiH3: Metastable SiSn/GeSn/Si(100) Heteroepitaxial Structures / J. Tolle, A.V.G. Chizmeshya, Y.-Y. Fang, J. Kouvetakis, V.R. D'Costa, C.-W. Hu, J. Menendez, I.S.T. Tsong // Appl. Phys. Lett. – 2006. – Vol. 89 (23). – P. 231924. doi:10.1063/1.2403903.
16. Oda M.Electronic Structure Calculation of $Si_{1-x}Sn_x$ Compound Alloy Using Interacting Quasi-Band Theory / M. Oda, Y. Kuroda, A. Kishi, Y. Shinozuka // Phys. Status Solidi B. – 2017. – Vol. 254 (2). – P. 1600519. doi:10.1002/pssb.201600519.
17. Nagae Y. Density Functional Study for Crystalline Structures and Electronic Properties of $Si_{1-x}Sn_x$ Binary Alloys / Y. Nagae, M. Kurosawa, S. Shibayama, M. Araidai, M. Sakashita, O. Nakatsuka, K. Shiraishi, S. Zaima // Jpn. J. Appl. Phys. – 2016. – Vol. 55 (8S2). – P. 08PE04. doi:10.7567/JJAP.55.08PE04.
18. Soref R. A. Predicted Band Gap of the New Semiconductor SiGeSn / R.A. Soref and C.H. Perry // Journal of Applied Physics. – 1991. – Vol. 69 (1). –P. 539–541.

doi:10.1063/1.347704.
19. Moontragoon P. Band Structure Calculations of Si–Ge–Sn Alloys: Achieving Direct Band Gap Materials / P. Moontragoon, Z. Ikonic, P. Harrison // Semicond. Sci. Technol. – 2007. – Vol. 22 (7). – P. 742–748. doi:10.1088/0268-1242/22/7/012.
20. Moontragoon P. Electronic Properties Calculation of $Ge_{1-x-y}Si{-}xSn_y$ Ternary Alloy and Nanostructure / P. Moontragoon, P. Pengpit, T. Burinprakhon, S. Maensiri, N. Vukmirovic, Z. Ikonic, P. Harrison // Journal of Non-Crystalline Solids. – 2012 . – Vol. 358 (17). – P. 2096–2098. doi:10.1016/j.jnoncrysol.2012.01.025.
21. Zhu Z. Composition-Dependent Band Gaps and Indirect–Direct Band Gap Transitions of Group-IV Semiconductor Alloys / Z. Zhu, J. Xiao, H. Sun, Y. Hu, R. Cao, Y. Wang, L. Zhao, J. Zhuang // Phys. Chem. Chem. Phys. – 2015. – Vol. 17 (33). – P. 21605–21610. doi:10.1039/C5CP02558C.
22. Ventura C. I. Electronic Structure of $Ge_{1-x-y}Si{-}xSn_y$ Ternary Alloys for Multijunction Solar Cells / C.I. Ventura, J.D. Querales Flores, J.D. Fuhr, R.A. Barrio // Prog. Photovolt: Res. Appl. – 2015. – Vol. 23 (1). – P. 112–118. doi:10.1002/pip.2405.
23. Fernando N. S. Band Gap and Strain Engineering of Pseudomorphic $Ge_{1-x-y}Si{-}xSn_y$ Alloys on Ge and GaAs for Photonic Applications / N.S. Fernando, R.A. Carrasco, R. Hickey, J. Hart, R. Hazbun, S. Schoeche, J.N. Hilfiker, J. Kolodzey, S. Zollner // Journal of Vacuum Science & Technology B, Nanotechnology and Microelectronics: Materials, Processing, Measurement, and Phenomena. – 2018. – Vol. 36 (2). – P. 021202. doi:10.1116/1.5001948.
24. Yakibchuk P. M. Model pseudopotential calculations for the electronic structure of Si, Ge, and GaAs / P. M. Yakibchuk, O. V. Bovgyra, I. V. Kutsa // J. Phys. Stud. – 2015. – Vol.19. – P. 1702 (7 p.).
25. Yakibchuk P. M. Nonlocal Model Pseudopotential Calculations of the Electronic Structure of AIIBVI (CdS, CdSe) Bulk Crystals and Nanocrystals / P.M. Yakibchuk, O.V. Bovgyra, L.R. Toporovska, I.V. Kutsa // J. Nano- Electron. Phys. – 2017. – Vol. 9 (2). – P. 02030–02037. doi:10.21272/jnep.9(2).02030.
26. Yakibchuk P. M. Electronic Structure of $Si_{1-x}Sn_x$ Disordered Solid Solutions / P.M. Yakibchuk, O.V. Bovgyra, M.V. Kovalenko, I.V. Kutsa // J. Phys. Stud. – 2019. – Vol. 23 (2). – P. 2703. doi:10.30970/jps.23.2703.
27. Weber J. Near-Band-Gap Photoluminescence of Si-Ge Alloys / J. Weber, M.I. Alonso // Phys. Rev. B. – 1989. – Vol. 40 (8). – P. 5683–5693. doi:10.1103/PhysRevB.40.5683.
28. Kurosawa M. Near-Infrared Light Absorption by Polycrystalline SiSn Alloys Grown on Insulating Layers / M. Kurosawa, M. Kato, T. Yamaha, N. Taoka, O. Nakatsuka, S. Zaima // Appl. Phys. Lett. – 2015. – Vol. 106 (17). – P. 171908. doi:10.1063/1.4919451.
29. Song, Z. Band Structure of $Ge_{1-x}Sn_x$ Alloy: A Full-Zone 30-Band k·p Model / // New J. Phys. – 2020. – Vol. 22 (1). – P. 019502.
30. He G. Interband Transitions in $Ge_{1-x}Sn_x$ Alloys / G. He, H.A. Atwater // Phys. Rev. Lett. – 1997. – Vol. 79 (10). – P. 1937–1940. doi:10.1088/1367-2630/ab6794.

References

1. R.A. Soref, Journal of Vacuum Science & Technology A: Vacuum, Surfaces, and Films **14**, 913 (1996). doi:10.1116/1.580414.
2. J. Kouvetakis, J. Menendez, and A.V.G. Chizmeshya, Annu. Rev. Mater. Res. **36**, 497 (2006). doi:10.1146/annurev.matsci.36.090804.095159.
3. A.M. Ionescu and H. Riel, Nature **479**, 329 (2011). doi:10.1038/nature10679.
4. C. Schulte-Braucks, S. Glass, E. Hofmann, D. Stange, N. von den Driesch, J.M. Hartmann, Z. Ikonic, Q.T. Zhao, D. Buca, and S. Mantl, Solid-State Electronics **128**, 54 (2017). doi:10.1016/j.sse.2016.10.024.
5. S. Wirths, D. Buca, and S. Mantl, Progress in Crystal Growth and Characterization of Materials **62**, 1 (2016). doi:10.1016/j.pcrysgrow.2015.11.001.
6. J. Shen, J. Zi, X. Xie, and P. Jiang, Phys. Rev. B **56**, 12084 (1997). doi:10.1103/PhysRevB.56.12084.
7. K. Alberi, J. Blacksberg, L.D. Bell, S. Nikzad, K.M. Yu, O.D. Dubon, and W. Walukiewicz, Phys. Rev. B **77**, 073202 (2008). doi:10.1103/PhysRevB.77.073202.
8. J.J. Pulikkotil, A. Chroneos, and U. Schwingenschogl, Journal of Applied Physics **110**, 036105 (2011). doi:10.1063/1.3618671.
9. K. Lu Low, Y. Yang, G. Han, W. Fan, and Y.-C. Yeo, Journal of Applied Physics **112**, 103715 (2012). doi:10.1063/1.4767381.
10. M.-H. Lee, P.-L. Liu, Y.-A. Hong, Y.-T. Chou, J.-Y. Hong, and Y.-J. Siao, Journal of Applied Physics **113**, 063517 (2013). doi:10.1063/1.4790362.
11. X. Wang, C. Chen, S. Feng, X. Wei, and Y. Li, Chinese Phys. B **26**, 127402 (2017). doi:10.1088/1674-1056/26/12/127402.
12. M.P. Polak, P. Scharoch, and R. Kudrawiec, J. Phys. D: Appl. Phys. **50**, 195103 (2017). doi:10.1088/1361-6463/aa67bf.
13. Y. Cho, S. Cho, B.-G. Park, and J.S. Harris, JSTS **17**, 675 (2017). doi:10.5573/JSTS.2017.17.5.675.
14. T.D. Eales, I.P. Marko, S. Schulz, E. O'Halloran, S. Ghetmiri, W. Du, Y. Zhou, S.-Q. Yu, J. Margetis, J. Tolle, E.P. O'Reilly, and S.J. Sweeney, Sci Rep **9**, 14077 (2019). doi:10.1038/s41598-019-50349-z.
15. J. Tolle, A.V.G. Chizmeshya, Y.-Y. Fang, J. Kouvetakis, V.R. D'Costa, C.-W. Hu, J. Menendez, and I.S.T. Tsong, Appl. Phys. Lett. **89**, 231924 (2006). doi:10.1063/1.2403903.
16. M. Oda, Y. Kuroda, A. Kishi, and Y. Shinozuka, Phys. Status Solidi B **254**, 1600519 (2017). doi:10.1002/pssb.201600519.
17. Y. Nagae, M. Kurosawa, S. Shibayama, M. Araidai, M. Sakashita, O. Nakatsuka, K. Shiraishi, and S. Zaima, Jpn. J. Appl. Phys. **55**, 08PE04 (2016). doi: 10.7567/JJAP.55.08PE04.
18. R.A. Soref and C.H. Perry, Journal of Applied Physics **69**, 539 (1991). doi:10.1063/1.347704.
19. P. Moontragoon, Z. Ikonic, and P. Harrison, Semicond. Sci. Technol. **22**, 742 (2007). doi:10.1088/0268-1242/22/7/012.

20. P. Moontragoon, P. Pengpit, T. Burinprakhon, S. Maensiri, N. Vukmirovic, Z. Ikonic, and P. Harrison, Journal of Non-Crystalline Solids **358**, 2096 (2012). doi:10.1016/j.jnoncrysol.2012.01.025.
21. Z. Zhu, J. Xiao, H. Sun, Y. Hu, R. Cao, Y. Wang, L. Zhao, and J. Zhuang, Phys. Chem. Chem. Phys. **17**, 21605 (2015). doi:10.1039/C5CP02558C.
22. C.I. Ventura, J.D. Querales Flores, J.D. Fuhr, and R.A. Barrio, Prog. Photovolt: Res. Appl. **23**, 112 (2015). doi:10.1002/pip.2405.
23. N.S. Fernando, R.A. Carrasco, R. Hickey, J. Hart, R. Hazbun, S. Schoeche, J.N. Hilfiker, J. Kolodzey, and S. Zollner, Journal of Vacuum Science & Technology B, Nanotechnology and Microelectronics: Materials, Processing, Measurement, and Phenomena **36**, 021202 (2018). doi:10.1116/1.5001948.
24. P. M. Yakibchuk, O. V. Bovgyra, I. V. Kutsa, J. Phys. Stud. **19**, 1702 (2015).
25. P.M. Yakibchuk, O.V. Bovgyra, L.R. Toporovska, I.V. Kutsa, J. Nano- Electron. Phys. **9**, 02030 (2017). doi:10.21272/jnep.9(2).02030.
26. P.M. Yakibchuk, O.V. Bovgyra, M.V. Kovalenko, and I.V. Kutsa, J. Phys. Stud. **23**, 2703 (2019). doi:10.30970/jps.23.2703.
27. J. Weber and M.I. Alonso, Phys. Rev. B **40**, 5683 (1989). doi:10.1103/PhysRevB.40.5683.
28. M. Kurosawa, M. Kato, T. Yamaha, N. Taoka, O. Nakatsuka, and S. Zaima, Appl. Phys. Lett. **106**, 171908 (2015). doi:10.1063/1.4919451.
29. Z. Song, W. Fan, C.S. Tan, Q. Wang, D. Nam, D.H. Zhang, and G. Sun, New J. Phys. **22**, 019502 (2020). doi:10.1088/1367-2630/ab6794.
30. G. He and H.A. Atwater, Phys. Rev. Lett. **79**, 1937 (1997). doi:10.1088/1367-2630/ab6794.

Статтю отримано: 13.02.2020
Прийнято до друку: 01.04.2020

Електронна енергетична структура твердих розчинів заміщення $Si_{1-x}Ge_x$, $Si_{1-x}Sn_x$ та $Ge_{1-x}Sn_x$

П.М. Якібчук, О.В. Бовгира, М.В. Коваленко, І.В. Куца

Львівський національний університет імені Івана Франка
вул. Кирила і Мефодія, 8, 79005 Львів, Україна
e-mail: oleh.bovhyra@lnu.edu.ua

Досліджено методом нелокального модельного псевдопотенціалу електронну енергетичну структуру твердих розчинів заміщення $Si_{1-x}Ge_x$, $Si_{1-x}Sn_x$ and $Ge_{1-x}Sn_x$. У цьому дослідженні ми моделювали низку суперкомірок, в яких атоми Si, Ge та Sn займали різні випадкові атомні позиції, що відповідає ідеальному гомогенному сплаву, тобто унеможлилює кластеризацію. Енергетичні діаграми структурних моделей розгянутих сполук були обчислені для усіх атомних конфігурацій з їх відповідною геометричною релаксацією. Тоді отримані значення енергетичних щілин усереднювали із врахуванням ймовірності формування відповідної структурної конфігурації. Додатково у розрахунках електронної енергетичної структури перелічених твердих розчинів заміщення враховано вплив внутрішніх локальних деформацій та композиційної невпорядкованості. Збіг результатів розрахунків для сполук $Si_{1-x}Ge_x$ (зокрема, зміна непрямої енергетичної щілини від точки X до L зони Бріллюена при 14% вмісту Si) із попередніми теоретичними та експериментальними дослідженнями демонструють надійність та адекватність використовуваного методу. Для $Ge_{1-x}Sn_x$ отриманий нами параметр оптичного прогину концентраційної залежності ширини прямої забороненої енергетичної щілини становить 2,74 еВ, а точка переходу із непрямозонного у прямозонний стан лежить при $x = 0,068$, що відповідає експериментальним даним. Встановлено, що перехід непрямозонний–прямозонний напівпровідник у сплавах $Si_{1-x}Sn_x$ відбувається за значення $x = 0,6$, а відповідне значення ширини прямої забороненої зони становить $E_g = 0{,}75$ еВ. Отримані композиційні залежності міжзонних віддалей твердих розчинів $Si_{1-x}Sn_x$ and $Ge_{1-x}Sn_x$ можуть бути використані для пояснення результатів експериментальних досліджень відповідних напівпровідникових сплавів. Також отримані результати закладають основу для подальших досліджень електронної структури, електричних та/або оптичних властивостей, моделювання квантових пристроїв та застосувань напівпровідникових тернарних сплавів Si-Ge-Sn.

Ключові слова: модельний псевдопотенціал, зонна структура, напівпровідники